Kochi Chapter

Indian Geotechnical Conference
IGC 2022
15th – 17th December, 2022, Kochi

Numerical Simulation Study on Detection of Subsurface Micro crack Using Active Infrared Thermography.

Mrityunjay Jaiswal [1*], Resmi Sebastian [1] and Ravibabu Mulaveesala [2]

[1]Department of Civil Engineering, Indian Institute of Technology Ropar, Rupnagar, Punjab, India, Pin-140001

[2]Centre for Sensors, instrumentation and cyber-physical Systems Engineering (SeNSE),

Indian Institute of Technology Delhi, Hauz Khas, New Delhi-110016

j.mrityunjay@outlook.com

Abstract

Bursting of brittle rock is an abrupt and violent phenomena of rock failure in high stress mines that results in many irreparable losses, including human lives. In general, large number of microcracks initiation and propagation in rocks lead to the spalling of rocks in underground construction therefore detection of microcracks and location of its amalgamation helps to adjudge the stability and to give the early warning indications. A simulation study has been carried out using FEM software to examine the potential of subsurface microcracks detection using pulse infrared (IR) thermography. Using this proposed method, the potential collapse location along with crack depth and size of rock can be estimated. A box shaped granite rock with artificially planted microcracks of different width and depth has been geometrically modelled. A 3D convective heat transfer equation along with coded pulse input has been used to check the detection potential. A phase mechanism was adopted for extracting the features based on fast Fourier transform technique using MATLAB code. Further, single pixel temperature profiles at the surface of sound zone and cracked zone of the test samples were compared. The proposed predictive analysis may help to reduce the casualty that is caused by rock burst.

Keywords

Active infrared thermography, Rock failure, Pulse thermography; Microcrack detection, Comsol.

1. Introduction

Rockburst is an acute engineering disaster that occurs in high stress mining areas or deep tunnels. It is a quick phenomenon in brittle rocks and can be a considerable menace to the safety of on-site workers and equipment. Occurrence of rock bursts in deep mines is predominantly due to the concentrated stress, when rock mass is disturbed by mining process. Numerous microcracks are generated inside the rock mass ahead of any rock burst and the density of microcrack is very high at the specific location from where a large crack starts. Researchers [1-3] have suggested that a threshold estimate for the long-term strength requirement of crystalline rocks can be made using the concept of microcracks and proper understanding of microcrack characteristics within the rock can give valuable perception into source mechanism of rockburst [4]. However due to the heterogeneity of the rocks and complex condition, detection of inherent subsurface microcracks and prediction of rockbursts at field have always beenvery difficult. In the initial investigations of microcrack assessment, researchers [5] used optical microscopes to investigate the appearance and structure of microcracks. As technology advanced, computed tomography (CT) [6], Scanning electron microscopy (SEM) [7] are also being used to calculate the microcrack density but all these methods only quantify the microcrack location after rock failure whereas evaluating the rockburst potential require quantification or detection before failure. *Lockner ,1993* [8] used acoustic emissions to study rock fracture and since then acoustic emission (AE) technique emerged as the most popular methodology used by researchers to determine the degree of cracking. However, background sounds and small AE activity with low frequencies (below 20 kHz) during the crack initiation stages make it difficult to measure signals with low amplitudes and the cracking source [9] whereas, attenuation problems are associated with high frequency emission in AE signals as they decay much faster.

In an effort to resolve the aforementioned problem, a simulation study has been conducted to examine the possibility of active infrared thermography which is a complete novel approach in the identification of microcracks in rocks. In past few years, numerous researchers [10-14] have surveyed rock masses using infrared thermography techniques, with a focus on the passive thermography. The fundamental physics underlying this technique is that the microcracks contain air between two surfaces, and there is a significant difference in the thermal properties, such as conductivity and specific heat capacity, of air and other minerals present in the rocks. Therefore, the portion of the rock mass with crack may get heated up fast and also cool down fast as compared to other sound regions. The technique of active thermography has not been employed in rocks till date, however, it has shown very good results in other materials like steel, carbon and fibre reinforced polymer [15-16]. Mulaveesala.R et.al [15] used pulse compression approach to detect the flaws in carbon fibre reinforced polymer.

With the advancement of computer simulation technology, it is possible to examine how rocks behave and how external factors affect their physical characteristics, with numerical simulations. Lie et.al,2011 [17] performed theoretical study using simulation on vertical finite crack detection. The pulse laser spot thermography was simulated and its effect on the low carbon steel block was analysed. For the present study, a pulse thermography has been adopted in which a coded pulse was assigned in a granite sample having artificially

planted microcracks of various dimensions at various depths with the help of an FEM tool. Phraseogram of the sample has also been developed to detect and highlight the cracks from the outcome image sequences of the result.

2. Simulation and modelling

The heat distribution process in our geometrically modelled granite rock, in which microcracks of various sizes and depths are artificially planted, is simulated using the finite element method (FEM) application COMSOL® in order to investigate the heat conduction in this granite rock. The thermal modules in the COMSOL Multiphysics ® are used to carry out the 3D simulations of heat distribution maps. The "Heat Transfer in Solids" module runs a thermal simulation by loading the heat source with varied excitation patterns and powers. The sample is given the opportunity to cool down due to surrounding air convection.

2.1 Model Geometry

A 3D rectangular box shaped granitic rock sample of dimensions, 150×150×300 mm as shown in *figure 1* has been s geometrically modelled and subsurface cracks were created inside the sample as thin blocks that contain air .The width and depth of the cracks were placed such that widths were varying from left to right and depths were varying from bottom to top as represented in *Figure 2* .In order to define all the internal blocks as a separation of surface or crack boundary, partition debonding were created. Generally, the length of the microcracks is comparatively larger than other two dimensions and their aspect ratios are approximately thousand and more. This property of microcrack distinguished them from voids and consequently kept the length of the crack constant as 10 mm and breadth as 50micron. In order to analyse the thermal characteristics at the surface due to the presence of internal cracks, point evolution was also enabled which evaluates the heat distribution with respect to time for desired point locations. The material and thermal properties like thermal conductivity, thermal heat capacity and emissivity of granite were manually added [17], mechanical properties like modulus of elasticity, Poisson's ratio were calculated by testing the sample in laboratory (*figure 3*). For numerically simulating the air, all properties were selected from COMSOL library .

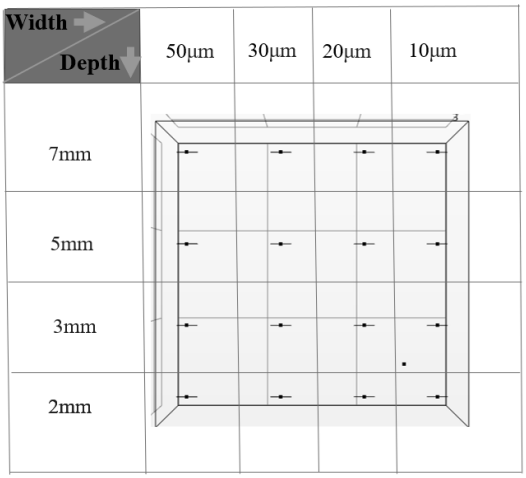

Figure 1 Outline diagram to represent location of microcracks

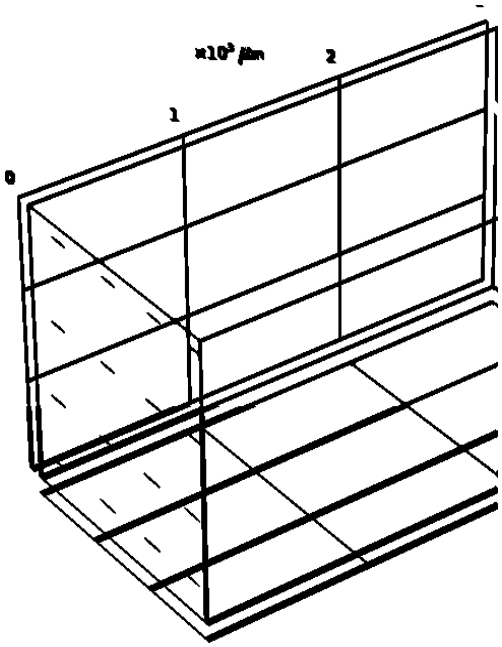

Figure 2 Schematic representation of granite sample with microcrack

.

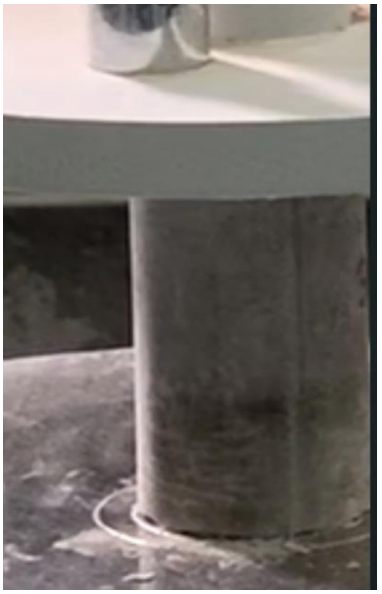

Figure 3 Basic property testing of sample

2.2 Mesh creation

A user-controlled random triangular mesh was defined (figure 4) for the geometry and meshing is considered as a crucial component in the finite element analyses for obtaining accurate results. Due to the vast differences in size between rock samples and fissures, two meshes with maximum and lowest element sizes of 600 microns and 10 microns each were established. The default values for the curvature factor and maximum element growth rate are 0.2 and 1.3, respectively. As such, quality measure was assessed using skewness on a scale of 0 to 1, as illustrated in figure 4. The ideal mesh is represented by a

skewness of 1, whereas the degraded mesh element is represented by skewness of 0. For the purposes of the current investigation, the created mesh was found to be sufficient.

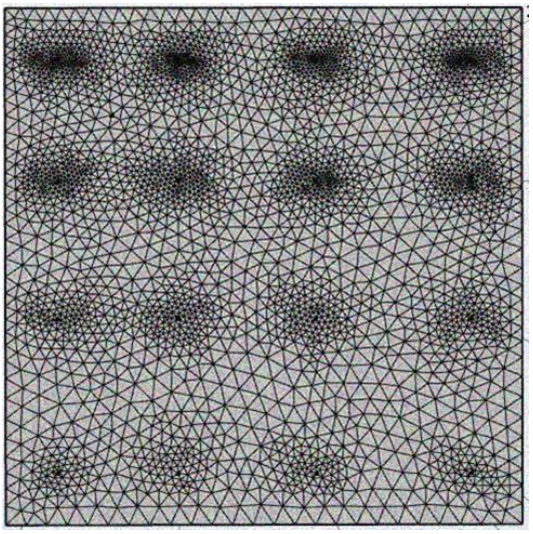

Figure 4 Mesh Generation

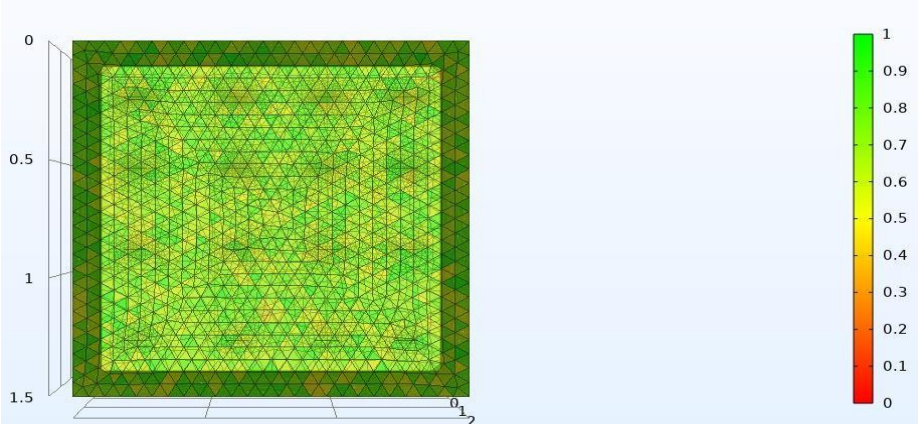

Figure 5 Mesh Quality

2.3 Heat transfer simulation

In active infrared thermography, pulse thermography (PT) and continuous wave lock-in thermography are very well recognised methods and widely used in many applications. Therefore, thermal response of the specimen with all sixteen subsurface microcracks were observed by imposing thermal excitation in the current simulation with a constant power of 1KW. The simulation used partial differential heat transfer equation as following.

$$\rho C\left(\frac{\partial T}{\partial t} + u.\nabla T\right) + \nabla.(-K.\nabla T) = Q_s \qquad (1)$$

Where, ρ is the density of specimen, C indicates heat capacity at constant pressure, k thermal conductivity, u is the velocity field. $Q_s$is the heat source (or sink), and T represents temperature.

As illustrated in figure 5 the front face and rare face heat fluxes were determined in terms of convection heat transfer and all other boundaries were considered to be insulated.

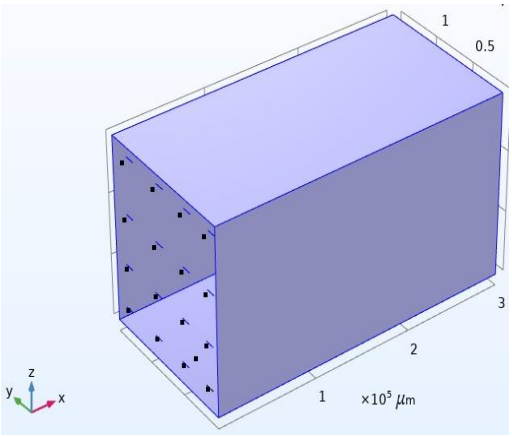

Figure 6 Thermally insulated surfaces

Mathematically,

$$C_x \frac{\partial T(x,y,z,t)}{\partial x} \vdots (x = 0) = C_x \frac{\partial T(x,y,z,t)}{\partial x} \vdots (x = l) = 0 \quad (2a)$$

$$C_y \frac{\partial T(x,y,z,t)}{\partial y} \vdots (y = 0) = C_x \frac{\partial T(x,y,z,t)}{\partial y} \vdots (y = b) = 0 \quad (2b)$$

$$C_x = C_y = C_z = C \quad (3)$$

Temperature distribution at initial condition at time t= 0 is taken as ambient temperature T_{am} (i.e. 293.1 K) which is given by,

$$T(x, y, z, t)|_{t=0} = T(x, y, z, 0) = T_{am}$$

2.3.1 Pulse infrared thermography

A coded long pulse heat flux with pulse width of 90 sec as shown in *figure 7* was imposed at the front face of the sample in which 40 sec was the heating period,50 sec was the cooling period and 1KW was the peak power. 10 Hz was the sampling frequency and pulse width was kept as the total sampling time.

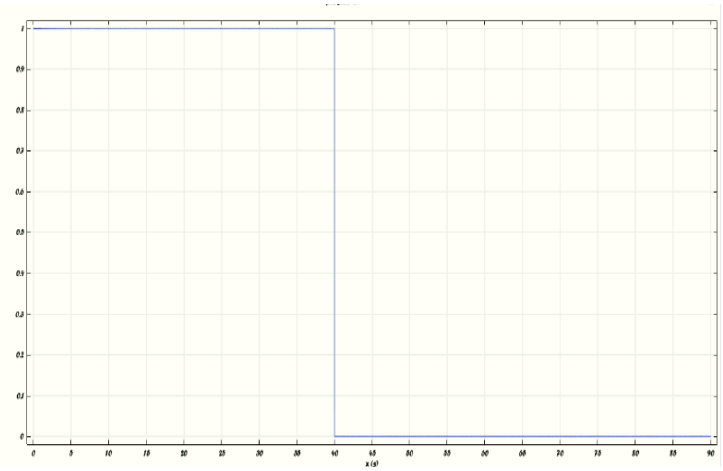

Figure 7 Pulse heat signal

3. Algorithm for post processing

The inhomogeneous non heating or emissivity prevents the detection of interior rock defects and this occasionally makes it difficult to detect the micron-sized inner defects using the temperature distribution image sequence of thermography. Therefore, a MATLAB algorithm was used to identify the flaws, to reduce the impact of uneven heating or emissivity on thermography detection as much as feasible and to enhance its fault identification capability. Fast Fourier transform (FFT) and principal component analysis (PCA) are the two common feature extraction approaches used in pulse thermal wave signals. In this study, a fast Fourier transform has been performed to convert the data from time domain to frequency domain and later on phase images were obtained by reconstructing the matrix into images.

4. Results and Discussions

4.1 single pixel profile

In infrared thermography, analysis can be carried out either by temperature curves or thermograms. *Figure 8* shows the single pixel profile at the surface of cracked zone and sound zone after pulse excitation and it was found that due to the presence of very small cracks, the temperature profile showed very minute differences at peak and cooling side limb. The thermal image sequence obtained from the simulation results were analysed. As can be seen in *figure 9*, the images obtained from PT give very minute contrasts in defect zone in absence of any post processing. However, after post processing, contrasts of the defect's region enhanced significantly as shown in figure 10, along with this the shape of the defect is also preserved. It was also observed that when a peak power of 1KW is applied to the specimen the maximum detectable depth of microcrack was 5 mm and minimum width it could detect was 10 microns. Either peak power or pulse width needed to be increased for detecting more deeper cracks.

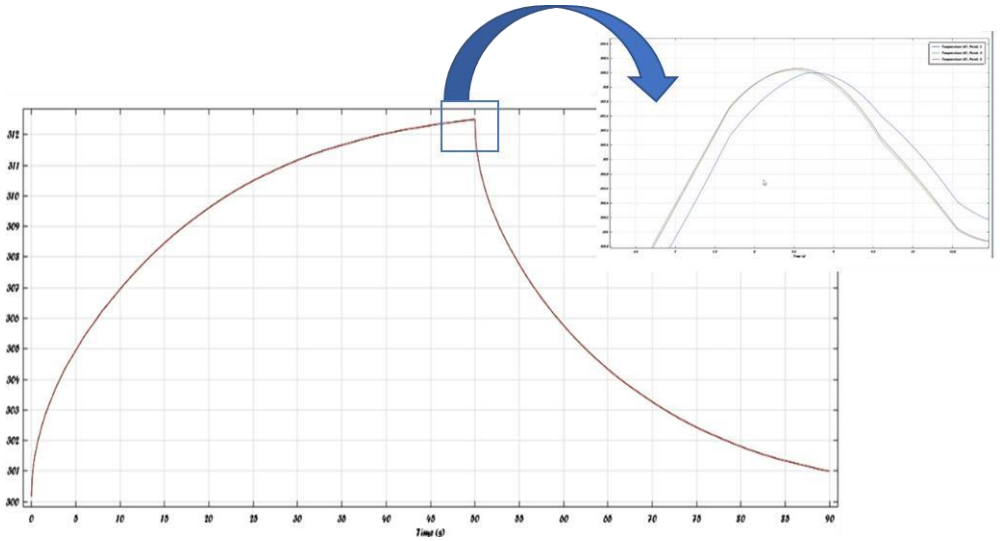

Figure 8 Single pixel profile -Pulse thermography

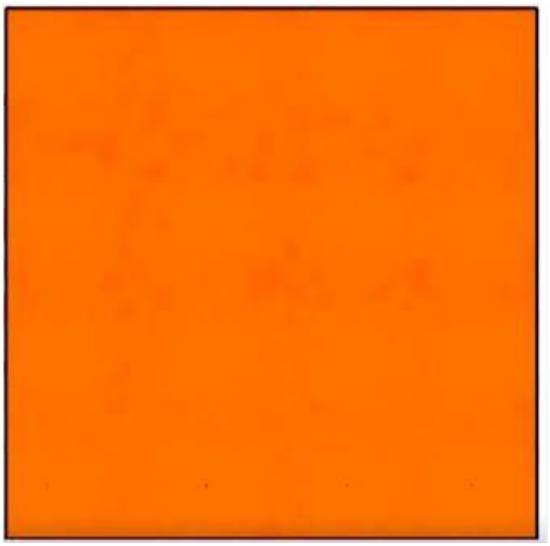

Figure 9 Thermal image output of pulse thermography at T=45s

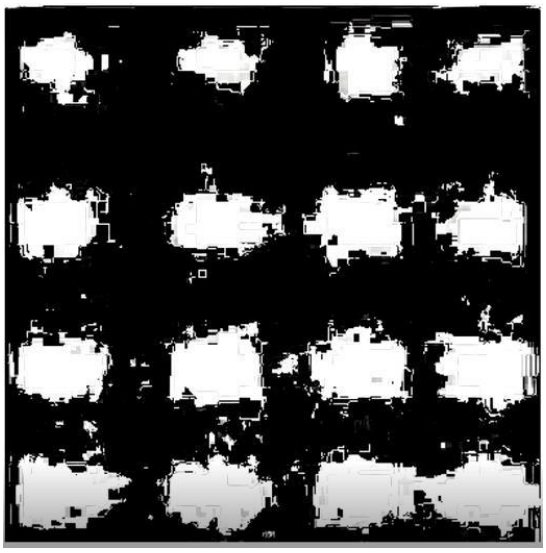

Figure 10 Post processed image output

4.2 Effect of crack tilt angle in the detection potential

Generally, microcracks are observed to be oriented in any random direction and in order to check the feasibility of this technique in practical situation, the angle of the cracks with respect to transverse plane were varied as 15°,30°,45°,60° and 75°. The observations were made after running the simulation for each individual sample and it was observed that for the power of 1KW, all the microcracks located at maximum depth of 25 mm, which were tilted up to 45-degree angle could be detected.

5. Conclusions

The simulation of active pulsed thermography, in a granitic sample with microcracks of different widths at different depths, has been conducted. 3D heat conduction model with external pulse heat was used in the simulation. The output image sequences have been optimized by phase analysis, which could enhance the defect detectability and the contrast, independent of non-uniform heating. The following conclusions can be drawn from this study.

1. The pulse thermography was numerically simulated, and it was found that for the microcracks located near to the surface, pulse phase thermography is effective and takes less observation time for the detection of microcracks.
2. The proposed algorithm for feature extraction is very effective in enhancing the contrast at defect zone.
3. It has been found that even a 45-degree tilted crack, located at far depth could also be detected in phase image of pulse thermography.

References

1) Liu, Qi, et al. "Experimental study on rock indentation using infrared thermography and acoustic emission techniques." Journal of Geophysics and Engineering 15.5 (2018): 1864-1877.
2) Rodríguez, Patricia, Paola B. Arab, and Tarcisio B. Celestino. "Characterization of rock cracking patterns in diametral compression tests by acoustic emission and petrographic analysis." International Journal of Rock Mechanics and Mining Sciences 83 (2016): 73-85.
3) Anders, Mark H., Stephen E. Laubach, and Christopher H. Scholz. "Microfractures: A review." Journal of Structural Geology 69 (2014): 377-394.
4) Qian, Qihu, and Xiaoping Zhou. "Quantitative analysis of rockburst for surrounding rocks and zonal disintegration mechanism in deep tunnels." Journal of Rock Mechanics and Geotechnical Engineering 3.1 (2011): 1-9.
5) Alm, Ove, Lise-Lotte Jaktlund, and Kuo Shaoquan. "The influence of microcrack density on the elastic and fracture mechanical properties of Stripa granite." Physics of the Earth and Planetary Interiors 40.3 (1985): 161-179.
6) Ge, Xiurun, et al. "Real-in time CT test of the rock meso-damage propagation law." Science in China Series E: Technological Sciences 44.3 (2001): 328-336.
7) Dengler, L. "Microcracks in crystalline rocks." Electron microscopy in mineralogy. Springer, Berlin, Heidelberg, 1976. 550-556.
8) D lockner
9) Nicksiar, Mohsen, and C. D. Martin. "Evaluation of methods for determining crack initiation in compression tests on low-porosity rocks." Rock mechanics and rock engineering 45.4 (2012): 607-617.
10) Kononov, V. A. Infrared thermography of loose hanging walls. Safety in Mines Research Advisory Committee GAP 820, 1–102 (2002).
11) W. Liu, S., Xu, Z., Wu, L., Ma, B. & Liu, X. Infrared Imaging Detection of Hidden Danger in Mine Engineering (In Progress in Electromagnetics Research Symposium Proceedings, Suzhou, China, 125–129, 2011).
12) Frodella, W., Morelli, S., Gigli, G. & Casagli, N. Contribution of infrared thermography to the slope instability characterization. In Proceedings of world landslide forum 3, 144–147 (2014).
13) Vogt, D., Brink, V. Z., Brink, S., Price, M. & Kagezi, B. New technology for improving entry examination, thereby managing the rockfall risk in south african gold and platinum mines (CSIR, Center for Mining Innovation, Auckland Park, Johannesburg, South Africa, 2010)
14) Prendes-Gero, M. B., Suárez-Domínguez, F. J., González-Nicieza, C. & Álvarez-Fernández, M. I. Infrared thermography methodology applied to detect localized rockfalls in self-supporting underground mines (In ISRM International SymposiumEUROCK 2013, International Society for Rock Mechanics, 2013)
15) Mulaveesala, Ravibabu, Jyani Somayajulu Vaddi, and Pushpraj Singh. "Pulse compression approach to infrared nondestructive characterization." Review of Scientific Instruments 79.9 (2008): 094901.
16) Watase, Azusa, et al. "Practical identification of favorable time windows for infrared thermography for concrete bridge evaluation." Construction and Building Materials 101 (2015): 1016-1030.

17) Li, Guo-hua, et al. "Numerical simulation of non-destructive testing of stainless-steel composites plate by infrared thermography." Journal of Shanghai Jiaotong University (Science) 16.3 (2011): 333-336.
18) Petrov, V. A., et al. "Microstructure, filtration, elastic and thermal properties of granite rock samples: implications for HLW disposal." Geological Society, London, Special Publications 240.1 (2005): 237-253.